

CHANSON, H. (2011). "Bubbly Two-Phase Flow in Hydraulic Jumps at Large Froude Numbers." *Journal of Hydraulic Engineering*, ASCE, Vol. 137, No. 4, pp. 451-460 (DOI: 10.1061/(ASCE)HY.1943-7900.0000323) (ISSN 0733-9429).

BUBBLY TWO-PHASE FLOW IN HYDRAULIC JUMPS AT LARGE FROUDE NUMBERS

Hubert Chanson

Professor in Civil Engineering, The University of Queensland, Brisbane QLD 4072, Australia, Ph.: (61 7) 3365 4163, Fax: (61 7) 3365 4599, E-mail: h.chanson@uq.edu.au

Abstract: A hydraulic jump is a sudden rapid transition from a super- to a sub-critical flow. At large inflow Froude numbers, the jump is characterised by a significant amount of entrained air. Herein the bubbly two-phase flow properties of steady and strong hydraulic jumps were investigated experimentally. The results demonstrate the strong air entrainment rate, and the depth-averaged void fraction data highlight a rapid de-aeration of the jump roller. The results suggest that the hydraulic jumps are effective aerators and that the rate of detrainment is comparatively smaller at the largest Froude numbers.

Keywords: Hydraulic jumps, Bubbly two-phase flow, Froude numbers, Physical modelling.

INTRODUCTION

The hydraulic jump is a classical flow situation defined as the rapid transition from a supercritical open channel flow to a subcritical flow. At prototype scales, the jump is characterised by a highly turbulent flow region with macro-scale vortices, that is called the roller, associated with significant kinetic energy dissipation and a bubbly two-phase flow region. Figures 1A and 1B show two photographs of hydraulic jumps for different inflow conditions highlighting the substantial aeration of the roller. The bubbly two-phase flow is caused by the strong interaction between the turbulence structures and the free surface at the impingement of the supercritical flow with the roller, leading to some air entrapment. Generally the air bubble entrainment takes place when the turbulent stresses overcome both surface tension and viscous forces (Ervin and Falvey 1987, Chanson 1997).

Bubbly flow measurements in hydraulic jumps were first performed by Rajaratnam (1962). Resch et al. (1974) and Babb and Aus (1981) conducted some hot-film probe measurements in the bubbly flow region and Resch et al. (1974) showed in particular the effects of upstream flow conditions of the air-water flow properties in the jump roller. Chanson (1995) highlighted the presence of a local maximum void fraction in the shear layer of hydraulic jumps with partially-developed inflow: that is, when the upstream flow is not fully-developed and turbulent boundary layer does not extend up to the free-surface. Chanson and Brattberg (2000) and Murzyn et al. (2005,2007) showed some seminal bubbly flow features in steady and weak hydraulic jumps respectively. Turbulence measurements in hydraulic jumps were conducted also by Rouse et al. (1959), Liu et al. (2004), Chanson (2007) and Kucukali and Chanson (2008), although the first study was conducted in a wind tunnel, and the second was restricted to low Froude numbers ($Fr_1 < 3.3$).

Despite all these advances, the knowledge into the bubbly two-phase flow region remains limited. The

present study examines in detail the two-phase flow properties in hydraulic jumps. The analysis is based upon some experimental results conducted in a relatively large facility covering a wide range of inflow Froude numbers. It is the aim of this work to characterise the bubbly flow properties in steady and strong hydraulic jumps.

Dimensional considerations

An experimental investigation performed with geometrically similar models must be based upon a sound similitude. For a hydraulic jump in a horizontal rectangular channel, a dimensional analysis shows that the parameters affecting the air-water flow properties at a position (x, y) include the fluid properties, the channel properties, and the inflow conditions properties (Wood 1991, Chanson 1997). After limited simplifications, it yields a series of dimensionless relationships in terms of the two-phase flow properties (Chanson and Gualtieri 2008):

$$C, \frac{F \times d_1}{V_1}, \frac{V}{V_1}, \dots = F \left(\frac{x - x_1}{d_1}, \frac{y}{d_1}, \frac{x_1}{d_1}, \frac{V_1}{\sqrt{g \times d_1}}, \frac{\rho \times V_1 \times d_1}{\mu}, \frac{g \times \mu^4}{\rho \times \sigma^3}, \frac{W}{d_1}, \frac{\delta}{d_1}, \dots \right) \quad (1)$$

where C is the void fraction, F is the bubble count rate, V is the velocity, x is the coordinate in the flow direction measured from the nozzle, y is the vertical coordinate, d_1 and V_1 are respectively the upstream flow depth and velocity, x_1 is the distance from the upstream gate, ρ , μ and σ are the water density, dynamic viscosity and surface tension respectively, W is the channel width and δ is the upstream boundary layer thickness (Fig. 2). Equation (1) expresses the dimensionless two-phase flow properties (left handside terms) at a dimensionless position $(x/d_1, y/d_1)$ within the roller as functions of the dimensionless inflow properties and channel geometry. In the right side, the 4th and 5th terms are the inflow Froude and Reynolds numbers respectively, and the 6th term is the Morton number. The Morton number is a function only of fluid properties and gravity constant. When water and air are used in both laboratory and prototype, the Morton number is invariant (Wood 1991, Crowe et al. 1998, Chanson 2009). The two key dimensionless parameters are the inflow Froude number $Fr_1 = V_1 / \sqrt{g \times d_1}$ and Reynolds number $Re = \rho \times q / \mu$ where q is the flow rate per unit width.

In an undistorted geometrically similar model of a hydraulic jump, the dynamic similarity is achieved if each dimensionless parameter has the same value in model and prototype. The turbulent processes and air entrainment in the shear region are dominated by viscous forces. Dynamic similarity of air entrainment in hydraulic jumps becomes impossible because the Froude and Reynolds numbers cannot be both equal in model and prototype, unless at full scale. A Froude similitude is commonly used in the study of hydraulic jump and the Reynolds numbers are typically smaller at laboratory conditions (Henderson 1966). A number of studies showed that the air entrainment in small size laboratory models might be drastically underestimated (Rao and Kobus 1971, Wood 1991, Chanson 1997). Some recent investigations performed some Froude similar experiments with $5.1 < Fr_1 < 8.5$ and Reynolds numbers between 2.4×10^4 and 9.8×10^4 (Chanson and Gualtieri 2008, Murzyn and Chanson 2008). The results showed some drastic scale effects in

CHANSON, H. (2011). "Bubbly Two-Phase Flow in Hydraulic Jumps at Large Froude Numbers." *Journal of Hydraulic Engineering*, ASCE, Vol. 137, No. 4, pp. 451-460 (DOI: 10.1061/(ASCE)HY.1943-7900.0000323) (ISSN 0733-9429).

the smaller hydraulic jumps ($Re < 4 \times 10^4$) in terms of the distributions of void fraction, bubble count rate and bubble size, but the issue of scale effects is still not settled.

EXPERIMENTAL FACILITY AND INSTRUMENTATION

The experiments were performed in a horizontal rectangular flume at the Gordon McKay Hydraulics Laboratory of University of Queensland. The channel length and width were 3.2 m and 0.50 m respectively. The sidewall height was 0.45 m. The sidewalls were made of 3.2 m long glass panels and the channel bed was in smooth PVC. This channel was previously used by Chanson (2007), Kucukali and Chanson (2008) and Murzyn and Chanson (2009). Photographs of the experimental facility are shown in Figure 1 and further details on the apparatus, instrumentation and data sets are reported in Chanson (2009b).

The water discharge was measured with a Venturi meter installed in the supply line and calibrated in-situ with a large V-notch weir. The discharge accuracy was within $\pm 2\%$. The clear-water flow depths were measured using rail mounted point gauges within 0.5 mm. The inflow conditions were controlled by a vertical gate with a semi-circular rounded shape ($\varnothing = 0.3$ m). The clear-water velocities were measured with a Prandtl-Pitot tube ($\varnothing = 3.02$ mm) based on the Prandtl design.

The two-phase flow properties were measured with a double-tip conductivity probe. The conductivity probe is a phase-detection intrusive probe designed to pierce the bubbles. It is based on the difference in electrical resistance between air and water (Crowe et al. 1998, Chanson 2002). In the present study, the probe was equipped with two identical sensors with an inner diameter of 0.25 mm. The distance between probe tips was $\Delta x = 6.96$ mm. The probe was manufactured at the University of Queensland and was previously used in several studies, including Kucukali and Chanson (2008). The displacement and the position of the probe in the vertical direction were controlled by a fine adjustment system connected to a Mitutoyo™ digimatic scale unit with a vertical accuracy Δy of less than 0.1 mm. The analysis of the probe signal output was based upon a single threshold technique and the threshold was set between 45% and 55% of the air-water voltage range. A number of two-phase flow properties were derived from the signal analysis. These include the void fraction C , or air concentration, defined as the volume of air per unit volume of air and water, the bubble count rate F defined as the number of bubbles impacting the probe tip per second, and the bubble chord size distribution. The air-water interfacial velocity V was estimated as $V = \Delta x/T$ where Δx is the longitudinal distance between both tips ($\Delta x = 6.96$ mm here) and T is the average air-water interfacial time between the two probe sensors with T being deduced from a cross-correlation analysis (Crowe et al. 1998, Chanson 1997,2002).

EXPERIMENTAL FLOW CONDITIONS

A first series of experiments investigated the general hydraulic jump properties, including upstream and downstream depths, and jump toe fluctuation frequency (Table 1). In the second series, some detailed two-phase flow measurements were performed using the double-tip probe, and the flow conditions are reported in

Table 1.

For all experiments, the jump toe was located at $x_1 = 0.75$ m and the same upstream rounded gate opening $h = 0.018$ m was used for the whole study. For these conditions, the inflow depth ranged from $d_1 = 0.0178$ to 0.019 m depending upon the flow rate (Table 1), and the inflow was characterised by a partially-developed boundary layer ($\delta/d_1 = 0.4$ to 0.6). Further the upstream flow was little aerated. Some vertical profiles of the void fraction were measured at a location 0.2 m upstream of the jump toe and the data show that the depth-averaged void fraction C_{mean} is less or equal to 0.11 , where C_{mean} is defined as:

$$C_{\text{mean}} = \int_0^{Y_{90}} C \times dy \quad (2)$$

with y the distance normal to the invert, C the local void fraction and Y_{90} the vertical distance from the bed where $C = 0.9$.

In the present study, the experiments are conducted primarily with large Froude numbers ($Fr_1 > 7$) and large Reynolds numbers ($Re > 5 \times 10^4$).

BASIC FLOW PATTERNS

A basic feature of hydraulic jumps is the rapid rise of the free surface immediately downstream of the jump toe. The free-surface is strongly turbulent with large vertical fluctuations and a bubbly/foamy structure as shown in Figure 1 for two Froude numbers. Figure 3 presents the ratio of the downstream to upstream depths d_2/d_1 as a function of the inflow Froude number Fr_1 . The experimental data are compared with the application of the equation of conservation of momentum:

$$\frac{d_2}{d_1} = \frac{1}{2} \times \left(\sqrt{1 + 8 \times Fr_1^2} - 1 \right) \quad (3)$$

where Fr_1 is the inflow Froude number. Equation (3) is compared with the experimental observations in Figure 3 illustrating a good agreement except at the largest Froude number. In that case ($Fr_1 = 11.2$), the jump roller interferes with the downstream overshoot gate.

The dimensionless roller length and bubbly flow region length are also presented in Figure 3. Herein the roller length L_r is defined as the location where the water surface was quasi-horizontal and the downstream depth is measured as sketched in Figure 2. The length L_{air} of the bubbly flow region was determined through some sidewall observations of the entrained air bubbles: i.e., L_{air} is the average length of the bubbly flow region. The present data are qualitatively in agreement with the correlations of Hager et al. (1990) and Murzyn et al. (2007) developed for $Fr_1 < 8$ and 5 respectively, although both correlations tended to underestimate the jump length by 20-30% (Fig. 3). For the present data set, L_r and L_{air} are best correlated by:

$$\frac{L_r}{d_1} = 13.7 \times Fr_1^{0.85} \quad 5.4 < Fr_1 < 12.4 \quad (4)$$

$$\frac{L_{\text{air}}}{d_1} = 9.54 \times Fr_1 - 9.1 \quad 5.4 < Fr_1 < 12.4 \quad (5)$$

CHANSON, H. (2011). "Bubbly Two-Phase Flow in Hydraulic Jumps at Large Froude Numbers." *Journal of Hydraulic Engineering*, ASCE, Vol. 137, No. 4, pp. 451-460 (DOI: 10.1061/(ASCE)HY.1943-7900.0000323) (ISSN 0733-9429).

The horizontal oscillations of the jump toe were recorded. These oscillations had relatively small amplitudes and their frequencies were estimated. The results are presented in Figure 4 in terms of the Strouhal number defined as $St = F_{toe} \times d_1 / V_1$ where F_{toe} is the toe oscillation frequency. The data are compared with some earlier studies of jump toe oscillations (Fig. 4). The present jump toe data yield in average $St \approx 0.005$ that are close to the findings of Mossa and Tolve (1998), Chanson (2007) and Murzyn and Chanson (2009). The comparative results show that there was no evident relationship between Strouhal and Reynolds numbers (Fig. 4).

BUBBLY FLOW PROPERTIES OF HYDRAULIC JUMPS

The hydraulic jumps are characterised by strong air bubble entrainment, spray and splashing (Fig. 1). Herein the two-phase flow measurements were conducted for five inflow Froude numbers ranging from 5.1 to 11.2 with a focus on the largest Froude numbers.

In hydraulic jumps with partially-developed inflow, the turbulent shear layer corresponds to an advective diffusion region in which the void fractions distributions exhibit a peak in the turbulent shear region (Resch et al. 1974, Chanson 1995). This is illustrated in Figures 5 and 6. Figure 5 presents some dimensionless distributions of void fraction along the hydraulic jump for two Froude numbers ($Fr_1 = 9.2$ and 11.2). The characteristic location Y_{90}/d_1 where the void fraction equals 0.90 is also shown (thick dashed line). It characterised the location of the roller's upper free-surface. Within the roller ($y < Y_{90}$), the void fraction profiles present a characteristic shape. The void fraction is about zero next to the invert. A local maximum ($C = C_{max}$) is observed in the shear layer as sketched in Figure 2. Close the free-surface, the void fraction increases rapidly towards unity.

In the air-water shear layer, the void fraction distributions follow closely an analytical solution of the advective diffusion equation for air bubbles (Chanson 1995):

$$C = C_{max} \times \exp \left(- \frac{1}{4 \times D^{\#}} \times \frac{\left(\frac{y - Y_{C_{max}}}{d_1} \right)^2}{\left(\frac{x - x_1}{d_1} \right)} \right) \quad (6)$$

where $D^{\#}$ is a dimensionless diffusivity: $D^{\#} = D_t / (V_1 \times d_1)$, D_t is the air bubble diffusivity, d_1 and V_1 are respectively the inflow depth and velocity, and $Y_{C_{max}}$ is the distance from the bed where $C = C_{max}$ (Fig. 2). Equation (6) is compared with some data in Figure 6 at four longitudinal locations in a hydraulic jump. The results illustrate the advective diffusion process with a broadening of the air-water shear region and the lesser maximum void fraction with increasing distance from the jump toe. Note that the void fraction is small at about mid-depth of the flow (Fig. 6). It is believed that this is related to the intense advective diffusion process at the largest Froude numbers: i.e., the air bubbles are advected downstream very rapidly and do not have time to migrate to the upper flow region. This yields a low void fraction layer between the air-water shear layer and the upper free-surface region as shown in Figure 6.

CHANSON, H. (2011). "Bubbly Two-Phase Flow in Hydraulic Jumps at Large Froude Numbers." *Journal of Hydraulic Engineering*, ASCE, Vol. 137, No. 4, pp. 451-460 (DOI: 10.1061/(ASCE)HY.1943-7900.0000323) (ISSN 0733-9429).

Figure 7 presents some dimensionless distributions of bubble count rate $F \times d_1 / V_1$ along the hydraulic jump for the same flow conditions shown in Figure 5. The characteristic location Y_{90} / d_1 is shown also. For any bubble shape and size distribution, the bubble count rate is proportional to the air-water interface area, and inversely proportional to the average bubble size for a given void fraction. It is simply proportional to the local rate of re-aeration. In the hydraulic jump roller, the vertical profiles of bubble count rate present a distinct, maximum count rate in the air-water shear layer: i.e., $y/d_1 \sim 1$ to 2 in Figure 7 depending upon the longitudinal location. The local maximum bubble count rate in the shear layer is believed to be linked with the region of maximum shear stress. Above, the bubble count rate decreases with increasing distance from the invert, and it is equal to zero for $C = 1$ (and $C = 0$).

Some two-phase velocity measurements were conducted in the bubbly flow region with the dual-tip probe based upon the mean interfacial travel time between the probe sensors ($\Delta x = 6.96$ mm). Some typical results are presented in Figure 8 for two Froude numbers ($Fr_1 = 7.5$ and 10.0). The graphs present the dimensionless vertical distributions of interfacial velocities V/V_1 in the hydraulic jump roller. The dimensionless location of the measurement section is given in the legend. At the channel bed, a no-slip condition imposes $V(y=0) = 0$. All the velocity profiles exhibit a similar shape despite some scatter. They follow the wall jet equations (Rajaratnam 1965, Chanson and Brattberg 2000). In the recirculation region above the shear layer, the present data indicate some negative time-averaged velocities (Fig. 8). While the probe design was not intended for some negative velocity measurements, the results show that the recirculation motion is qualitatively observed with the dual-tip probe.

The bubble chord size measurements show a broad spectrum of bubble sizes at each location. The range of bubble sizes extend over several orders of magnitude from less than 0.5 mm to more than 20 mm. Their distributions are skewed with a preponderance of small bubbles relative to the mean. In Figures 9A and 9B corresponding to the air-water shear region, the probability of bubble size is the largest for chord times between 0 and 0.5 mm although the mean size was between 2 and 6 mm. The probability distribution functions of bubble size followed typically a log-normal distribution; a similar finding was observed by Resch et al. (1974) and Chanson (2007). Figure 9 shows some typical normalised bubble chord size distributions in the developing shear layer. For each graph, the caption provides the location $(x-x_1, y/d_1)$, the local air-water flow properties (C, F, V) and the average bubble size. The histogram columns represent each the probability of droplet chord time in a 0.5 mm chord interval. For example, the probability of bubble chord from 1 to 1.5 mm is represented by the column labelled 1 mm. Bubble sizes larger than 10 mm are regrouped in the last column (> 10 mm).

DISCUSSION

In the design of hydraulic structures and stilling basins, a relevant design parameter is the depth-averaged void fraction and the rate of air entrainment. In some cases, the flow aeration must be maximised: e.g., for re-oxygenation purposes. In others situations, it must be prevented or reduced: e.g., effect of flow bulking on sidewall heights. In each case, the amount of air entrainment and the air-water flow properties must be

CHANSON, H. (2011). "Bubbly Two-Phase Flow in Hydraulic Jumps at Large Froude Numbers." *Journal of Hydraulic Engineering*, ASCE, Vol. 137, No. 4, pp. 451-460 (DOI: 10.1061/(ASCE)HY.1943-7900.0000323) (ISSN 0733-9429).

accurately predicted to optimise the system performances and to insure a safe operation.

Figure 10 presents the longitudinal distributions of depth-averaged void fraction C_{mean} in the hydraulic jump. C_{mean} is defined by Equation (2) and characterises the amount of entrained air since $C_{\text{mean}} = Q_{\text{air}}/(Q+Q_{\text{air}})$ where Q is the water discharge and Q_{air} is the rate of air entrainment. The present data show consistently a large rate of air entrainment in the jump as well as a rapid de-aeration of the flow with increasing distance from the jump toe (Fig. 10A). For the present data set, the longitudinal decay in depth-averaged void fraction is best correlated by:

$$C_{\text{mean}} = 0.3387 \times Fr_1^{0.202} * \exp\left(-0.103 + 0.0073 \times Fr_1\right) \times \frac{x - x_1}{d_1} \quad (7)$$

Equation (7) is compared with the present data set in Figure 10B. The agreement is reasonable with a normalised correlation coefficient of 0.947. The results imply a depth-averaged void fraction proportional to $Fr_1^{1/5}$ as well as a lower de-aeration rate with increasing Froude number. That is, the rate of detrainment is comparatively smaller at the largest Froude numbers (Fig. 10A & Eq. (5)).

For comparison, the experimental data of Rajaratnam (1962) and Mossa and Tolve (1998) are shown in Figure 10A where they are compared with the present data set. Note that Rajaratnam (1962) and Mossa and Tolve (1998) calculated their mean void fraction as an arithmetic mean rather than using Equation (2). The arithmetic mean is not a true depth-averaged void fraction (Eq. (2)).

CONCLUSION

Some detailed two-phase flow measurements were conducted in steady and strong hydraulic jumps with partially-developed inflow. The measurements of jump toe fluctuations are close to earlier studies. The void fraction distributions present a local maximum in the air-water shear layer where the distributions of void fractions are modelled by an advective diffusion equation. The shear zone is also characterised by a maximum in bubble count rate. The experimental observations highlight a strong air entrainment rate. The depth-averaged void fraction data demonstrate a large amount of entrained air as well as a rapid de-aeration of the jump roller, although the de-aeration is comparatively smaller at the largest Froude numbers.

The results suggest that the hydraulic jumps are effective aerators and that the dimensionless air content is retained longer at the largest Froude numbers, and thus these jumps are better suited for use as an aeration device.

ACKNOWLEDGEMENTS

The author thanks Ben Hopkins and Hugh Cassidy (The University of Queensland) who conducted carefully the experimental measurements. He further acknowledges the financial support of the Australian Research Council (Grant DP0878922).

CHANSON, H. (2011). "Bubbly Two-Phase Flow in Hydraulic Jumps at Large Froude Numbers." *Journal of Hydraulic Engineering*, ASCE, Vol. 137, No. 4, pp. 451-460 (DOI: 10.1061/(ASCE)HY.1943-7900.0000323) (ISSN 0733-9429).

REFERENCES

- Babb, A.F., and Aus, H.C. (1981). "Measurements of Air in Flowing Water." *Jl of Hyd. Div.*, ASCE, Vol. 107, No. HY12, pp. 1615-1630.
- Chanson, H. (1995). "Air Entrainment in Two-dimensional Turbulent Shear Flows with Partially Developed Inflow Conditions." *Intl Jl of Multiphase Flow*, Vol. 21, No. 6, pp. 1107-1121.
- Chanson, H. (1997). "Air Bubble Entrainment in Free-Surface Turbulent Shear Flows." *Academic Press*, London, UK, 401 pages.
- Chanson, H. (2002). "Air-Water Flow Measurements with Intrusive Phase-Detection Probes. Can we Improve their Interpretation ?" *Journal of Hydraulic Engineering*, ASCE, Vol. 128, No. 3, pp. 252-255.
- Chanson, H. (2007). "Bubbly Flow Structure in Hydraulic Jump." *European Journal of Mechanics B/Fluids*, Vol. 26, No. 3, pp.367-384 (DOI: 10.1016/j.euromechflu.2006.08.001).
- Chanson, H. (2009a). "Turbulent Air-water Flows in Hydraulic Structures: Dynamic Similarity and Scale Effects." *Environmental Fluid Mechanics*, Vol. 9, No. 2, pp. 125-142 (DOI: 10.1007/s10652-008-9078-3).
- Chanson, H. (2009b). "Advective Diffusion of Air Bubbles in Hydraulic Jumps with Large Froude Numbers: an Experimental Study." *Hydraulic Model Report No. CH75/09*, School of Civil Engineering, The University of Queensland, Brisbane, Australia, 89 pages & 3 videos.
- Chanson, H., and Brattberg, T. (2000). "Experimental Study of the Air-Water Shear Flow in a Hydraulic Jump." *Intl Jl of Multiphase Flow*, Vol. 26, No. 4, pp. 583-607.
- Chanson, H., and Gualtieri, C. (2008). "Similitude and Scale Effects of Air Entrainment in Hydraulic Jumps." *Journal of Hydraulic Research*, IAHR, Vol. 46, No. 1, pp. 35-44.
- Crowe, C., Sommerfield, M., and Tsuji, Y. (1998). "Multiphase Flows with Droplets and Particles." *CRC Press*, Boca Raton, USA, 471 pages.
- Ervine, D.A., and Falvey, H.T. (1987). "Behaviour of Turbulent Water Jets in the Atmosphere and in Plunge Pools." *Proc. Instn Civ. Engrs., London*, Part 2, Mar. 1987, 83, pp. 295-314.
- Hager, W.H., Bremen, R., and Kawagoshi, N. (1990). "Classical Hydraulic Jump: Length of Roller." *Jl of Hyd. Res.*, IAHR, Vol. 28, No. 5, pp. 591-608.
- Henderson, F.M. (1966). "Open Channel Flow." *MacMillan Company*, New York, USA.
- Kucukali, S., and Chanson, H. (2008). "Turbulence Measurements in Hydraulic Jumps with Partially-Developed Inflow Conditions." *Experimental Thermal and Fluid Science*, Vol. 33, No. 1, pp. 41-53 (DOI: 10.1016/j.expthermflusci.2008.06.012).
- Liu, M., Rajaratnam, N., and Zhu, D.Z. (2004). "Turbulent Structure of Hydraulic Jumps of Low Froude Numbers." *Jl of Hyd. Engrg.*, ASCE, Vol. 130, No. 6, pp. 511-520.
- Long, D., Rajaratnam, N., Steffler, P.M., and Smy, P.R. (1991). "Structure of Flow in Hydraulic Jumps." *Jl of Hyd. Research*, IAHR, Vol. 29, No. 2, pp. 207-218.
- Mossa, M., and Tolve, U. (1998). "Flow Visualization in Bubbly Two-Phase Hydraulic Jump." *Jl Fluids Eng.*, ASME, Vol. 120, March, pp. 160-165.

- CHANSON, H. (2011). "Bubbly Two-Phase Flow in Hydraulic Jumps at Large Froude Numbers." *Journal of Hydraulic Engineering*, ASCE, Vol. 137, No. 4, pp. 451-460 (DOI: 10.1061/(ASCE)HY.1943-7900.0000323) (ISSN 0733-9429).
- Murzyn, F., and Chanson, H. (2008). "Experimental Assessment of Scale Effects Affecting Two-Phase Flow Properties in Hydraulic Jumps." *Experiments in Fluids*, Vol. 45, No. 3, pp. 513-521 (DOI: 10.1007/s00348-008-0494-4).
- Murzyn, F., and Chanson, H. (2009). "Free-Surface Fluctuations in Hydraulic Jumps: Experimental Observations." *Experimental Thermal and Fluid Science*, Vol. 33, No. 7, pp. 1055-1064 (DOI: 10.1016/j.expthermflusci.2009.06.003)
- Murzyn, F., Mouaze, D., and Chaplin, J.R. (2005). "Optical Fibre Probe Measurements of Bubbly Flow in Hydraulic Jumps" *Intl Jl of Multiphase Flow*, Vol. 31, No. 1, pp. 141-154.
- Murzyn, F., Mouaze, D., and Chaplin, J.R. (2007). "Air-Water Interface Dynamic and Free Surface Features in Hydraulic Jumps." *Jl of Hydraulic Res.*, IAHR, Vol. 45, No. 5, pp. 679-685.
- Rajaratnam, N. (1962). "An Experimental Study of Air Entrainment Characteristics of the Hydraulic Jump." *Jl of Instn. Eng. India*, Vol. 42, No. 7, March, pp. 247-273.
- Rajaratnam, N. (1965). "The Hydraulic Jump as a Wall Jet." *Jl of Hyd. Div.*, ASCE, Vol. 91, No. HY5, pp. 107-132. Discussion : Vol. 92, No. HY3, pp. 110-123 & Vol. 93, No. HY1, pp. 74-76.
- Rao, N.S.L., and Kobus, H.E. (1971). "Characteristics of Self-Aerated Free-Surface Flows." *Water and Waste Water/Current Research and Practice*, Vol. 10, Eric Schmidt Verlag, Berlin, Germany.
- Resch, F.J., Leutheusser, H.J., and Alemu, S. (1974). "Bubbly Two-Phase Flow in Hydraulic Jump." *Jl of Hyd. Div.*, ASCE, Vol. 100, No. HY1, pp. 137-149.
- Rouse, H., Siao, T.T., and Nagaratnam, S. (1959). Turbulence Characteristics of the Hydraulic Jump." *Transactions*, ASCE, Vol. 124, pp. 926-950
- Wood, I.R. (1991). "Air Entrainment in Free-Surface Flows." *IAHR Hydraulic Structures Design Manual No. 4*, Hydraulic Design Considerations, Balkema Publ., Rotterdam, The Netherlands, 149 pages.

NOTATION

- C void fraction defined as the volume of air per unit volume of air and water;
- C_{\max} local maximum in void fraction in the developing shear layer;
- C_{mean} depth averaged void fraction:
- $$C_{\text{mean}} = \int_0^{Y_{90}} C \times dy$$
- D_t air bubble diffusivity (m^2/s) in the air-water shear layer;
- $D^\#$ dimensionless air bubble diffusivity: $D^\# = D_t / (V_1 \times d_1)$;
- d_1 flow depth (m) measured immediately upstream of the hydraulic jump;
- F bubble count rate (Hz) defined as the number of bubbles impacting the probe sensor per second;
- F_{\max} maximum bubble count rate (Hz) in the air-water shear layer;
- F_{toe} hydraulic jump toe oscillation frequency (Hz);
- Fr_1 upstream Froude number: $Fr_1 = V_1 / \sqrt{g \times d_1}$;

CHANSON, H. (2011). "Bubbly Two-Phase Flow in Hydraulic Jumps at Large Froude Numbers." *Journal of Hydraulic Engineering*, ASCE, Vol. 137, No. 4, pp. 451-460 (DOI: 10.1061/(ASCE)HY.1943-7900.0000323) (ISSN 0733-9429).

g	gravity acceleration (m/s^2) : $g = 9.80 \text{ m/s}^2$ in Brisbane (Australia);
h	sluice gate opening (m);
K	dimensionless constant;
L_{air}	hydraulic jump bubbly flow region length (m);
Q	water discharge (m^3/s);
Q_{air}	air flow rate (m^3/s);
Re	Reynolds number: $Re = \rho \times V_1 \times d_1 / \mu$;
T	average air-water interfacial travel time (s) between the two probe sensors;
V	air-water velocity (m/s);
V_1	upstream flow velocity (m/s): $V_1 = Q/(W \times d_1)$;
W	channel width (m);
x	longitudinal distance from the upstream sluice gate (m);
x_1	longitudinal distance from the upstream gate to the jump toe (m);
$Y_{C_{\text{max}}}$	vertical elevation (m) where the void fraction in the shear layer is maximum ($C = C_{\text{max}}$);
$Y_{F_{\text{max}}}$	distance (m) from the bed where the bubble count rate is maximum ($F = F_{\text{max}}$);
Y_{90}	characteristic distance (m) from the bed where $C = 0.90$;
y	distance (m) measured normal to the flow direction;
Δx	longitudinal distance (m) between probe sensors;
δ	boundary layer thickness (m);
μ	dynamic viscosity (Pa.s) of water;
ρ	density (kg/m^3) of water.

CHANSON, H. (2011). "Bubbly Two-Phase Flow in Hydraulic Jumps at Large Froude Numbers." *Journal of Hydraulic Engineering*, ASCE, Vol. 137, No. 4, pp. 451-460 (DOI: 10.1061/(ASCE)HY.1943-7900.0000323) (ISSN 0733-9429).

Table 1 - Experimental flow conditions

Ref.	Q	W	x_1	V_1	d_1	Fr_1	Re	Remarks
(1)	m^3/s (2)	m (3)	m (4)	m/s (5)	m (6)	(7)	(8)	(9)
Series 1								General observations
2	0.0147	0.5	0.75	1.55	0.019	3.58	2.9E+4	
3	0.0166	0.5	0.75	1.75	0.019	4.05	3.3E+4	
1	0.02225	0.5	0.75	2.34	0.019	5.42	4.4E+4	
5	0.0282	0.5	0.75	3.13	0.018	7.46	5.6E+4	
4	0.03255	0.5	0.75	3.52	0.0185	8.26	6.5E+4	
6	0.0367	0.5	0.75	4.08	0.018	9.70	7.3E+4	
7	0.0399	0.5	0.75	4.43	0.018	10.55	7.9E+4	
8	0.0470	0.5	0.75	5.22	0.018	12.43	9.3E+4	
Series 2								Two-phase flow measurements
090331	0.02025	0.5	0.75	2.19	0.0185	5.14	4.0E+4	
090317	0.02825	0.5	0.75	3.14	0.018	7.47	5.6E+4	
090720	0.03481	0.5	0.75	3.87	0.018	9.21	6.9E+4	
090713	0.03780	0.5	0.75	4.20	0.018	10.0	7.5E+4	
090414	0.04175	0.5	0.75	4.68	0.01783	11.2	8.3E+4	

Table 2 - Probability distribution functions of bubble chords in the shear layer for $Fr_1 = 11.2$, $Re = 8.3 \times 10^4$, $d_1 = 0.01783$ m, $x_1 = 0.75$ m (Fig. 9)

$x-x_1$ (m)	y/d_1	V (m/s)	C	F (Hz)	Average chord size (mm)	No. bubbles
0.225	1.04	3.09	0.217	189.1	3.78	8510
	1.32	2.90	0.351	211.9	5.73	9540
	1.60	2.78	0.382	194.2	5.97	8740
0.400	0.76	2.90	0.101	133.8	2.19	6020
	1.32	2.78	0.198	180.8	3.10	8140
	1.88	2.28	0.207	158.0	3.00	7110

CHANSON, H. (2011). "Bubbly Two-Phase Flow in Hydraulic Jumps at Large Froude Numbers." *Journal of Hydraulic Engineering*, ASCE, Vol. 137, No. 4, pp. 451-460 (DOI: 10.1061/(ASCE)HY.1943-7900.0000323) (ISSN 0733-9429).

LIST OF CAPTIONS

Fig. 1 - Air entrainment in hydraulic jumps

(A) $Fr_1 = 7.5$, $Re = 5.6 \times 10^4$, $d_1 = 0.018$ m, $x_1 = 0.75$ m, $x-x_1 = 0.150$ m, shutter speed: 1/80 s

(B) $Fr_1 = 10.0$, $Re = 7.5 \times 10^4$, $d_1 = 0.018$ m, $x_1 = 0.75$ m, $x-x_1 = 0.350$ m, shutter speed: 1/80 s

Fig. 2 - Definition sketch of the bubbly two-phase flow region in hydraulic jumps

Fig. 3 - Ratio of the conjugate depths d_2/d_1 , dimensionless roller length L_r/d_1 and bubble flow region length L_{air}/d_1 as functions of the inflow Froude number Fr_1 - Comparison between experimental data and the solution of the momentum equation

Fig. 4 - Jump toe oscillations: Strouhal number data

Fig. 5 - Dimensionless distribution of void fraction C - Horizontal axis: $0.1 \times (x-x_1)/d_1 + C$

(A) $Fr_1 = 9.2$, $Re = 6.9 \times 10^4$, $d_1 = 0.018$ m, $x_1 = 0.75$ m

(B) $Fr_1 = 11.2$, $Re = 8.3 \times 10^4$, $d_1 = 0.01783$ m, $x_1 = 0.75$ m

Fig. 6 - Void fraction distributions in a hydraulic jump with partially-developed inflow conditions: $x_1 = 0.75$ m, $d_1 = 0.018$ m, $Fr_1 = 9.2$, $Re = 6.9 \times 10^4$, $x-x_1 = 0.225, 0.30, 0.45$ and 0.60 m- Comparison between experimental data (Present study) and mathematical solution

(A, Left) $x-x_1 = 0.225$ m; (B, Right) $x-x_1 = 0.35$ m

(C, Left) $x-x_1 = 0.45$ m; (D, Right) $x-x_1 = 0.60$ m

Fig. 7 - Dimensionless distribution of bubble count rate $F \times d_1/V_1$ - Horizontal axis: $0.1 \times (x-x_1)/d_1 + F \times d_1/V_1$

(A) $Fr_1 = 9.2$, $Re = 6.9 \times 10^4$, $d_1 = 0.018$ m, $x_1 = 0.75$ m

(B) $Fr_1 = 11.2$, $Re = 8.3 \times 10^4$, $d_1 = 0.01783$ m, $x_1 = 0.75$ m

Fig. 8 - Dimensionless velocity distributions V/V_1 in hydraulic jumps - Horizontal axis: $0.1 \times (x-x_1)/d_1 + V/V_1$

(A) $Fr_1 = 7.5$, $Re = 5.6 \times 10^4$, $d_1 = 0.018$ m, $x_1 = 0.75$ m

(B) $Fr_1 = 10.0$, $Re = 7.5 \times 10^4$, $d_1 = 0.018$ m, $x_1 = 0.75$ m

CHANSON, H. (2011). "Bubbly Two-Phase Flow in Hydraulic Jumps at Large Froude Numbers." *Journal of Hydraulic Engineering*, ASCE, Vol. 137, No. 4, pp. 451-460 (DOI: 10.1061/(ASCE)HY.1943-7900.0000323) (ISSN 0733-9429).

Fig. 9 - Probability distribution functions of bubble chords in the shear layer: $Fr_1 = 11.2$, $Re = 8.3 \times 10^4$, $d_1 = 0.01783$ m, $x_1 = 0.75$ m - Flow characteristics summarised in Table 2

(A) $x - x_1 = 0.225$ m

(B) $x - x_1 = 0.400$ m

Fig. 10 - Dimensionless longitudinal distributions of depth-averaged void fraction C_{mean} in hydraulic jumps

(A) Comparison between the present data and previous studies (Rajaratnam 1962, Mossa and Tolve 1998)

(B) Comparison between experimental data and Equation (7)

CHANSON, H. (2011). "Bubbly Two-Phase Flow in Hydraulic Jumps at Large Froude Numbers." *Journal of Hydraulic Engineering*, ASCE, Vol. 137, No. 4, pp. 451-460 (DOI: 10.1061/(ASCE)HY.1943-7900.0000323) (ISSN 0733-9429).

Fig. 1 - Air entrainment in hydraulic jumps

(A) $Fr_1 = 7.5$, $Re = 5.6 \times 10^4$, $d_1 = 0.018$ m, $x_1 = 0.75$ m, $x - x_1 = 0.150$ m, shutter speed: 1/80 s



(B) $Fr_1 = 10.0$, $Re = 7.5 \times 10^4$, $d_1 = 0.018$ m, $x_1 = 0.75$ m, $x - x_1 = 0.350$ m, shutter speed: 1/80 s



CHANSON, H. (2011). "Bubbly Two-Phase Flow in Hydraulic Jumps at Large Froude Numbers." *Journal of Hydraulic Engineering*, ASCE, Vol. 137, No. 4, pp. 451-460 (DOI: 10.1061/(ASCE)HY.1943-7900.0000323) (ISSN 0733-9429).

Fig. 2 - Definition sketch of the bubbly two-phase flow region in hydraulic jumps

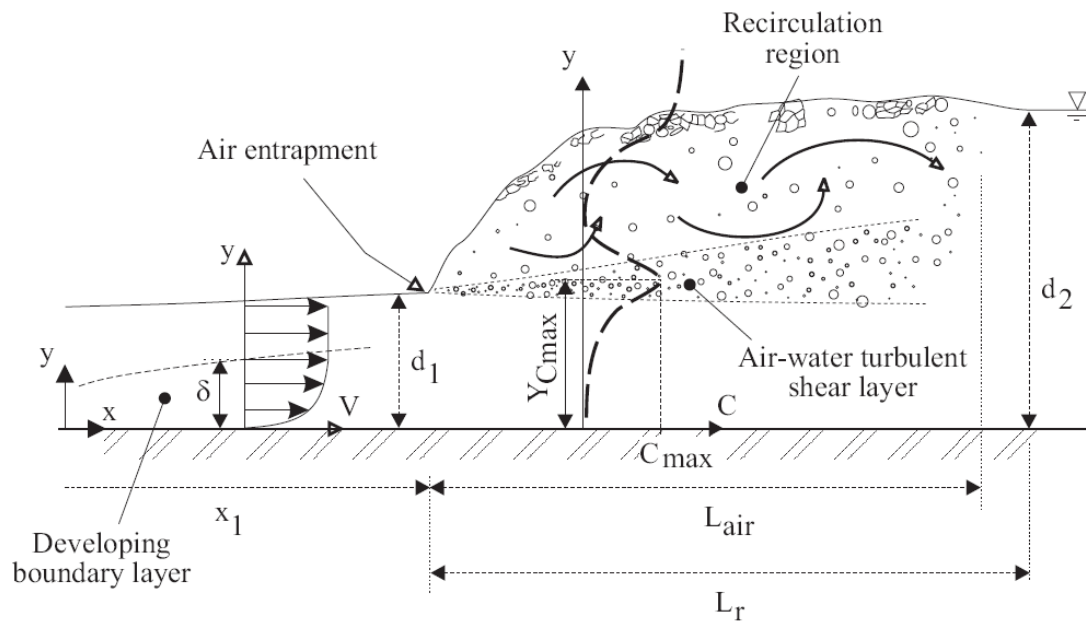


Fig. 3 - Ratio of the conjugate depths d_2/d_1 , dimensionless roller length L_r/d_1 and bubble flow region length L_{air}/d_1 as functions of the inflow Froude number Fr_1 - Comparison between experimental data and the solution of the momentum equation

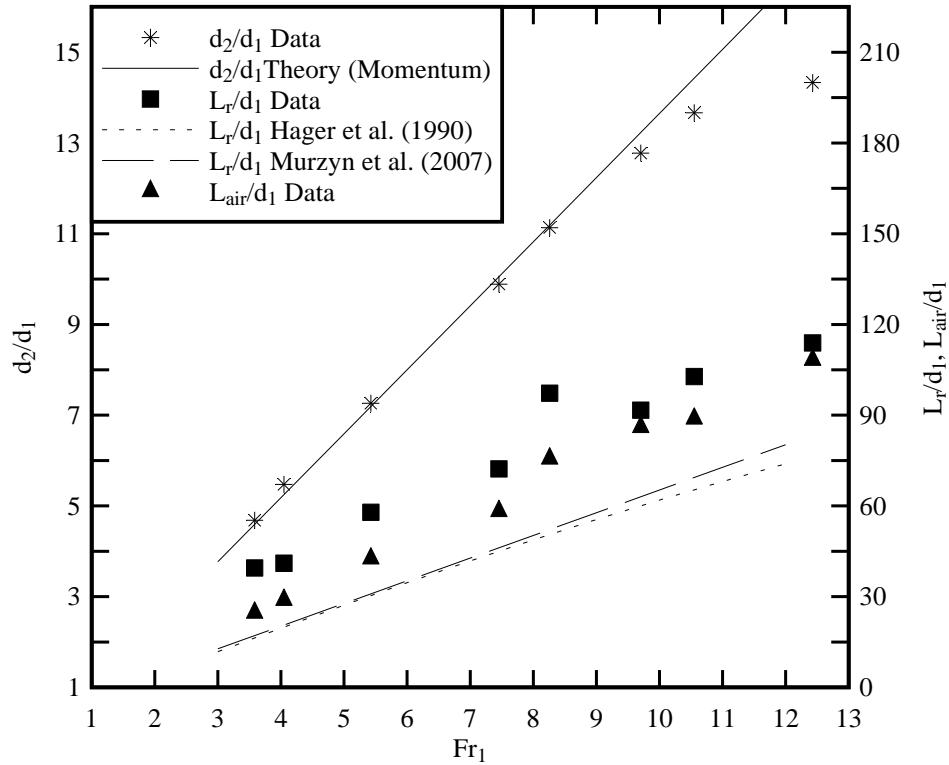


Fig. 4 - Jump toe oscillations: Strouhal number data

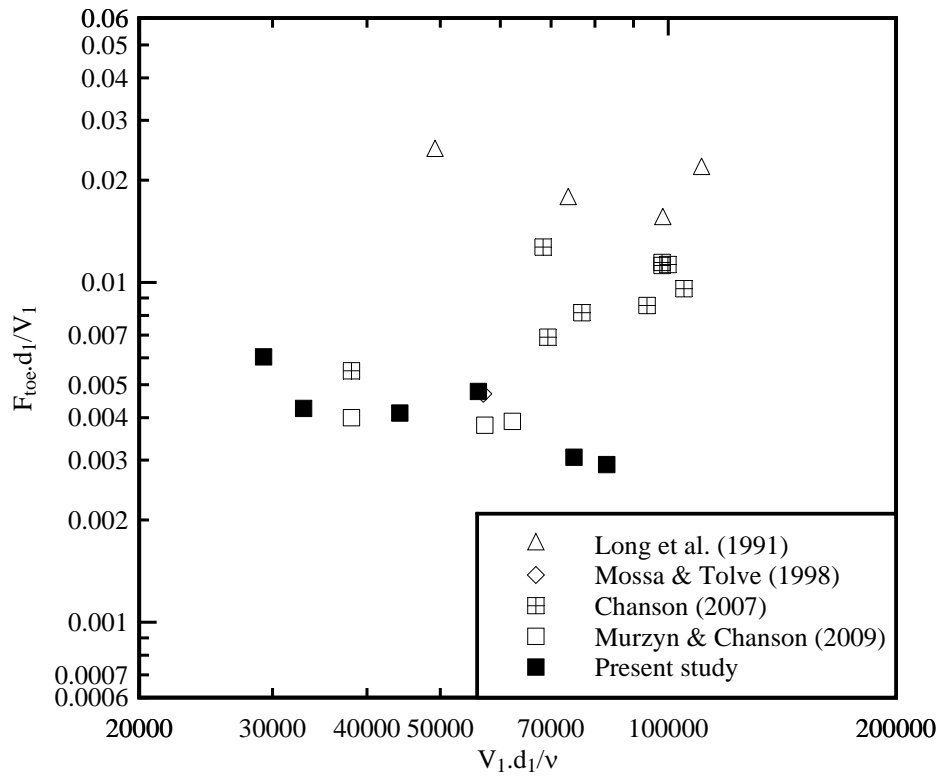
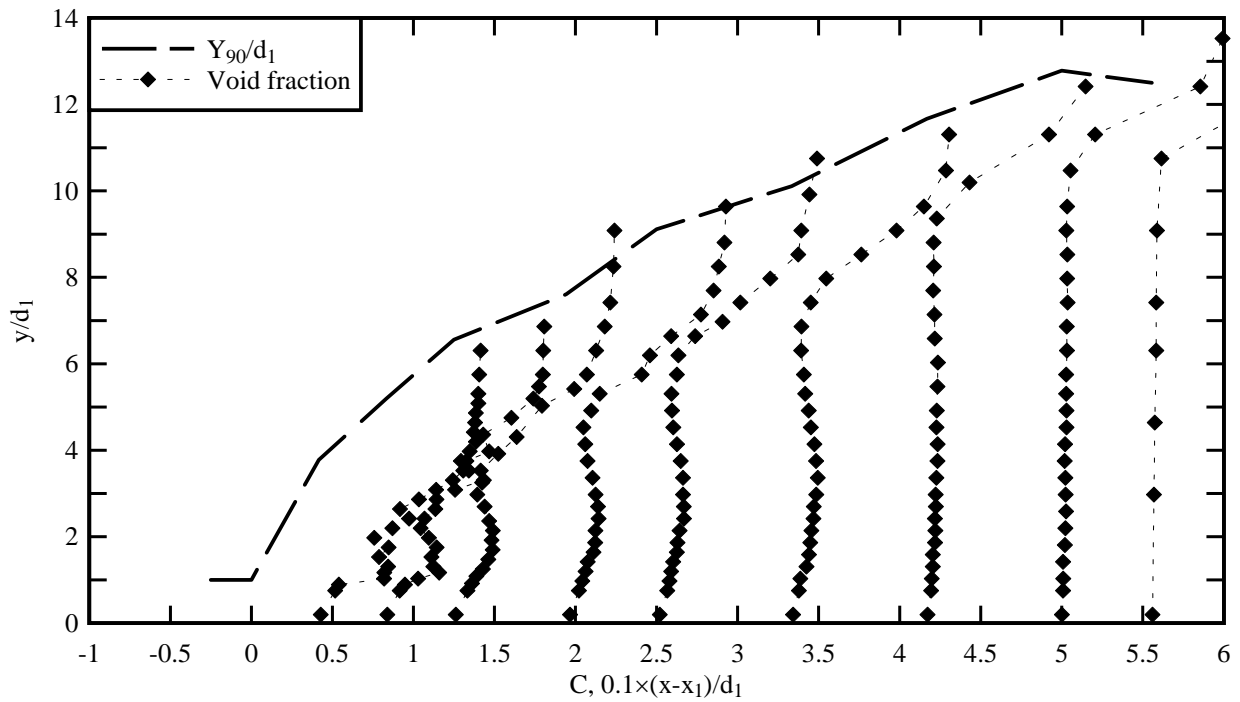


Fig. 5 - Dimensionless distribution of void fraction C - Horizontal axis: $0.1 \times (x - x_1) / d_1 + C$

(A) $Fr_1 = 9.2$, $Re = 6.9 \times 10^4$, $d_1 = 0.018$ m, $x_1 = 0.75$ m



(B) $Fr_1 = 11.2$, $Re = 8.3 \times 10^4$, $d_1 = 0.01783$ m, $x_1 = 0.75$ m

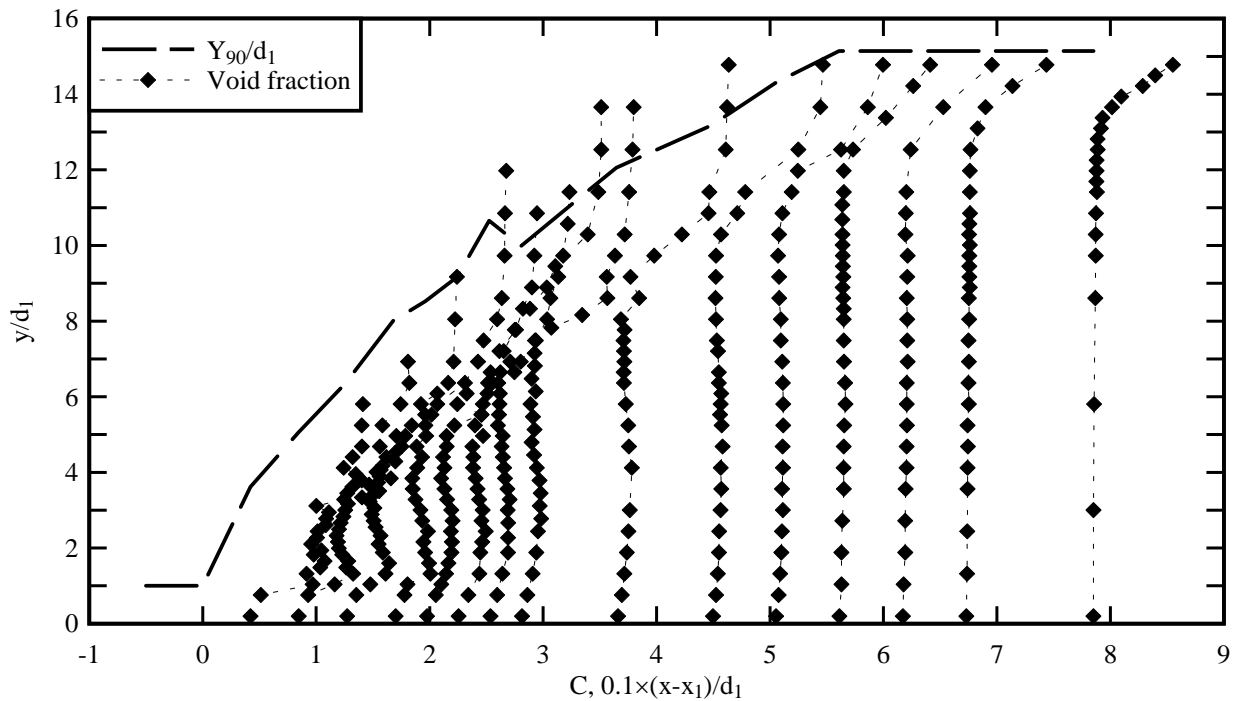
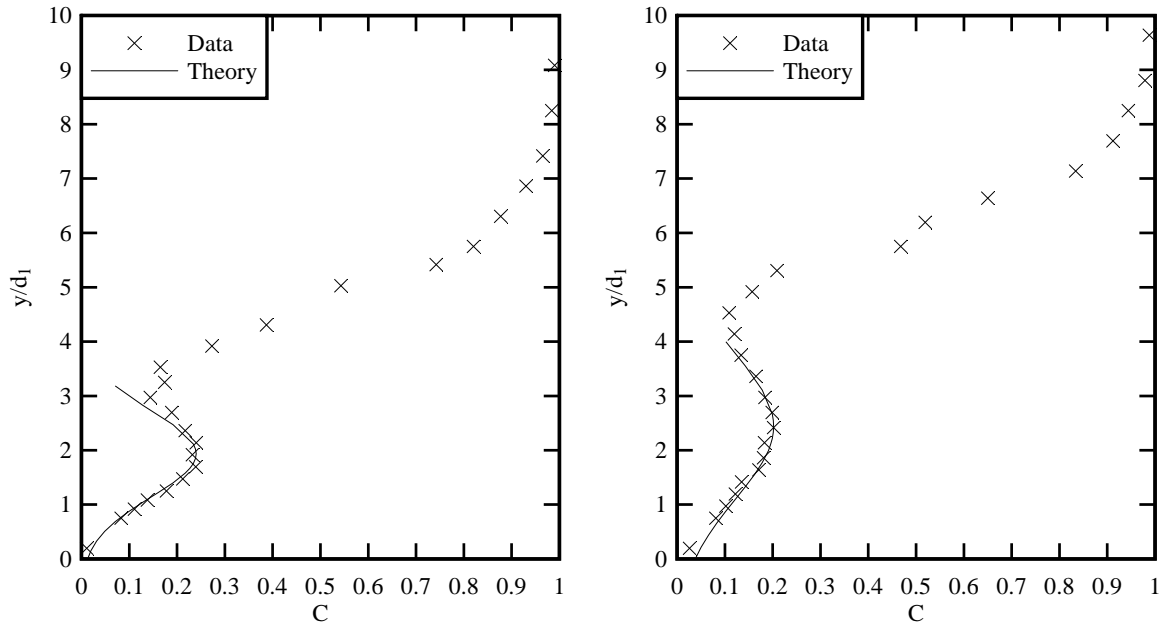


Fig. 6 - Void fraction distributions in a hydraulic jump with partially-developed inflow conditions: $x_1 = 0.75$ m, $d_1 = 0.018$ m, $Fr_1 = 9.2$, $Re = 6.9 \times 10^4$, $x - x_1 = 0.225, 0.30, 0.45$ and 0.60 m- Comparison between experimental data (Present study) and mathematical solution

(A, Left) $x - x_1 = 0.225$ m; (B, Right) $x - x_1 = 0.35$ m



(C, Left) $x - x_1 = 0.45$ m; (D, Right) $x - x_1 = 0.60$ m

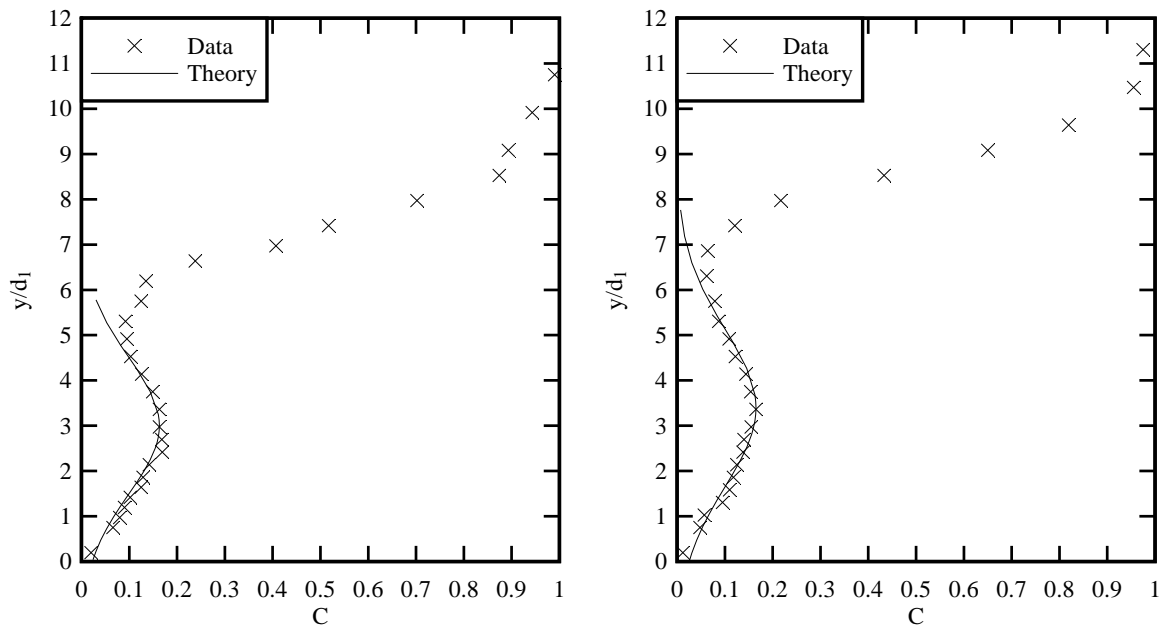
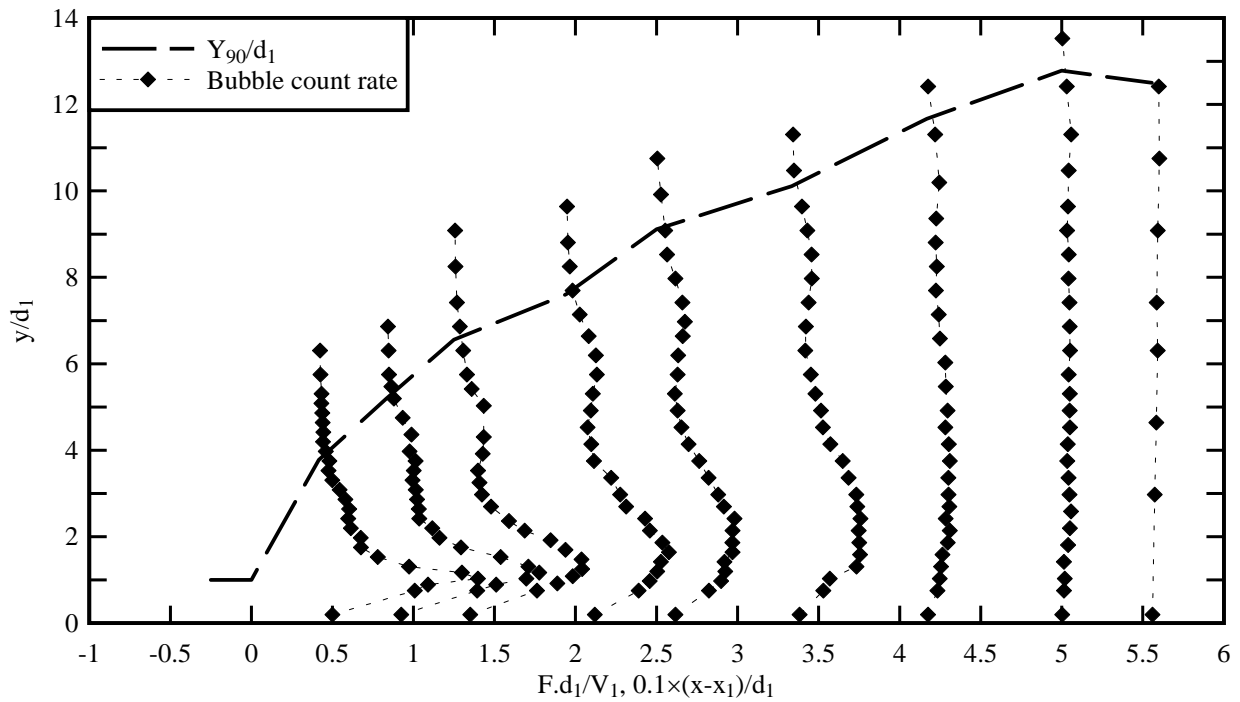


Fig. 7 - Dimensionless distribution of bubble count rate $F \times d_1 / V_1$ - Horizontal axis: $0.1 \times (x - x_1) / d_1 + F \times d_1 / V_1$

(A) $Fr_1 = 9.2$, $Re = 6.9 \times 10^4$, $d_1 = 0.018$ m, $x_1 = 0.75$ m



(B) $Fr_1 = 11.2$, $Re = 8.3 \times 10^4$, $d_1 = 0.01783$ m, $x_1 = 0.75$ m

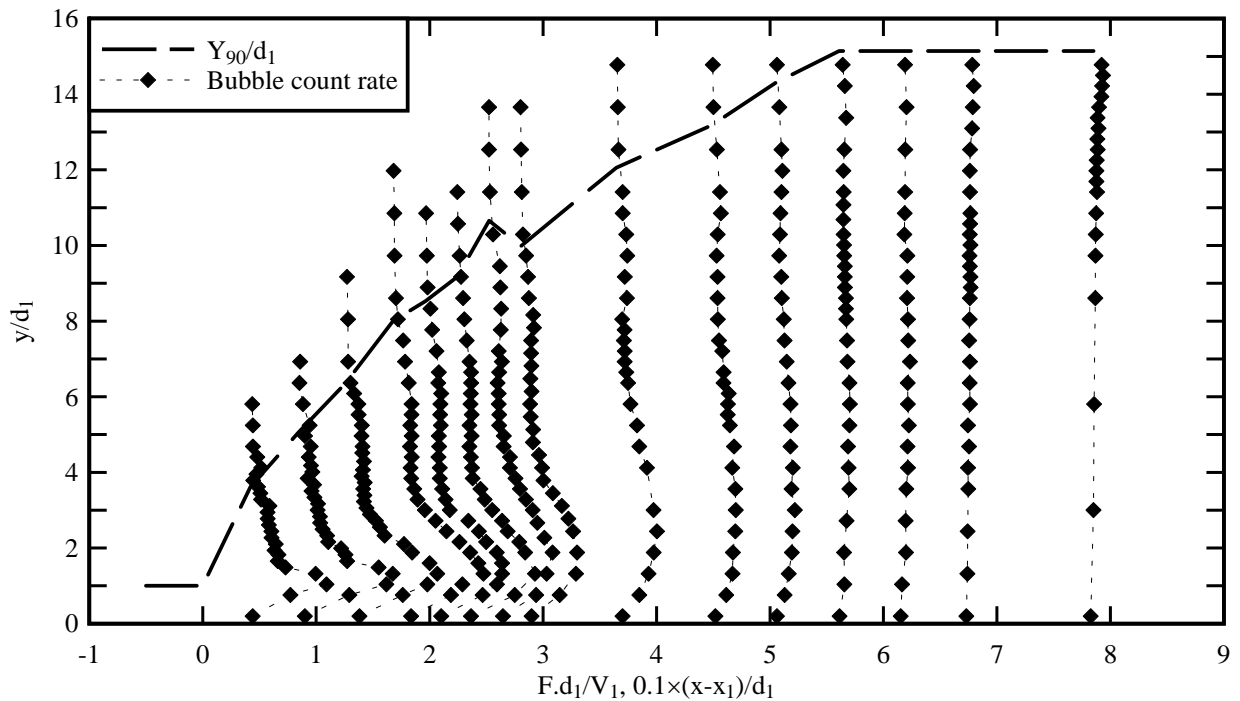
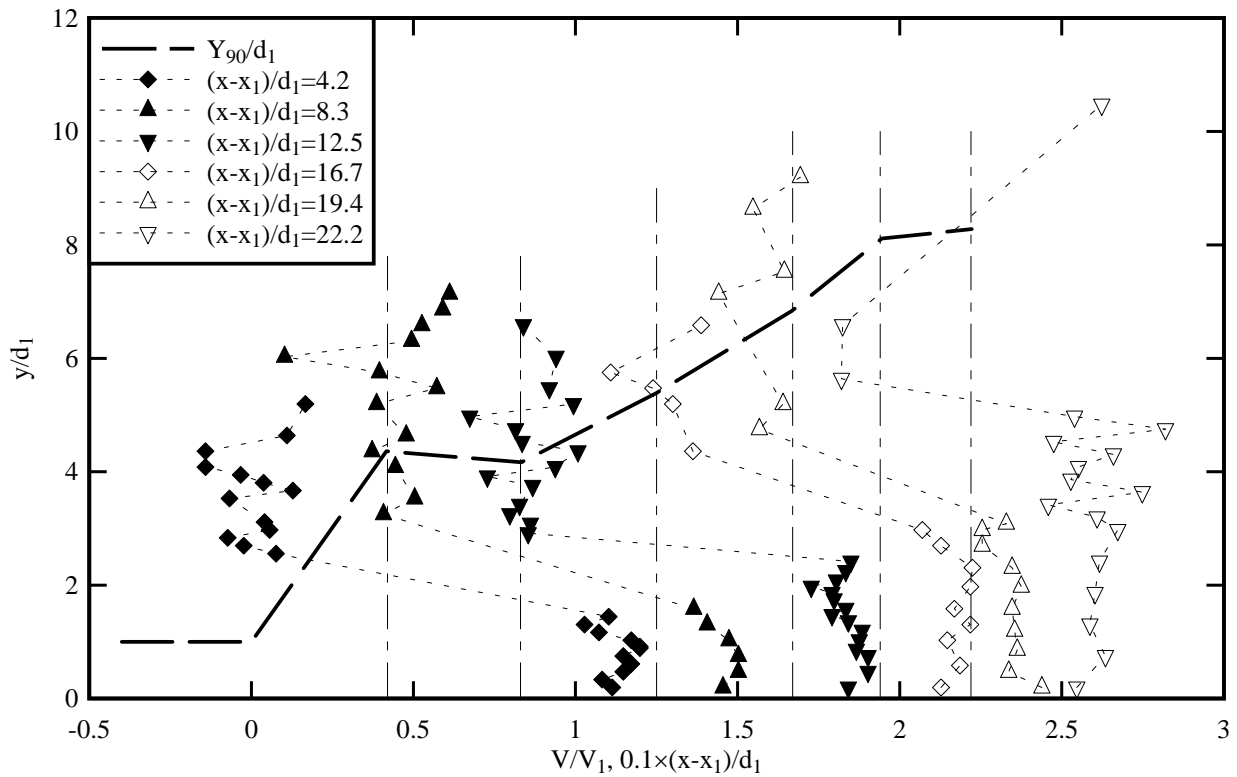


Fig. 8 - Dimensionless velocity distributions V/V_1 in hydraulic jumps - Horizontal axis: $0.1 \times (x-x_1)/d_1 + V/V_1$

(A) $Fr_1 = 7.5$, $Re = 5.6 \times 10^4$, $d_1 = 0.018$ m, $x_1 = 0.75$ m



(B) $Fr_1 = 10.0$, $Re = 7.5 \times 10^4$, $d_1 = 0.018$ m, $x_1 = 0.75$ m

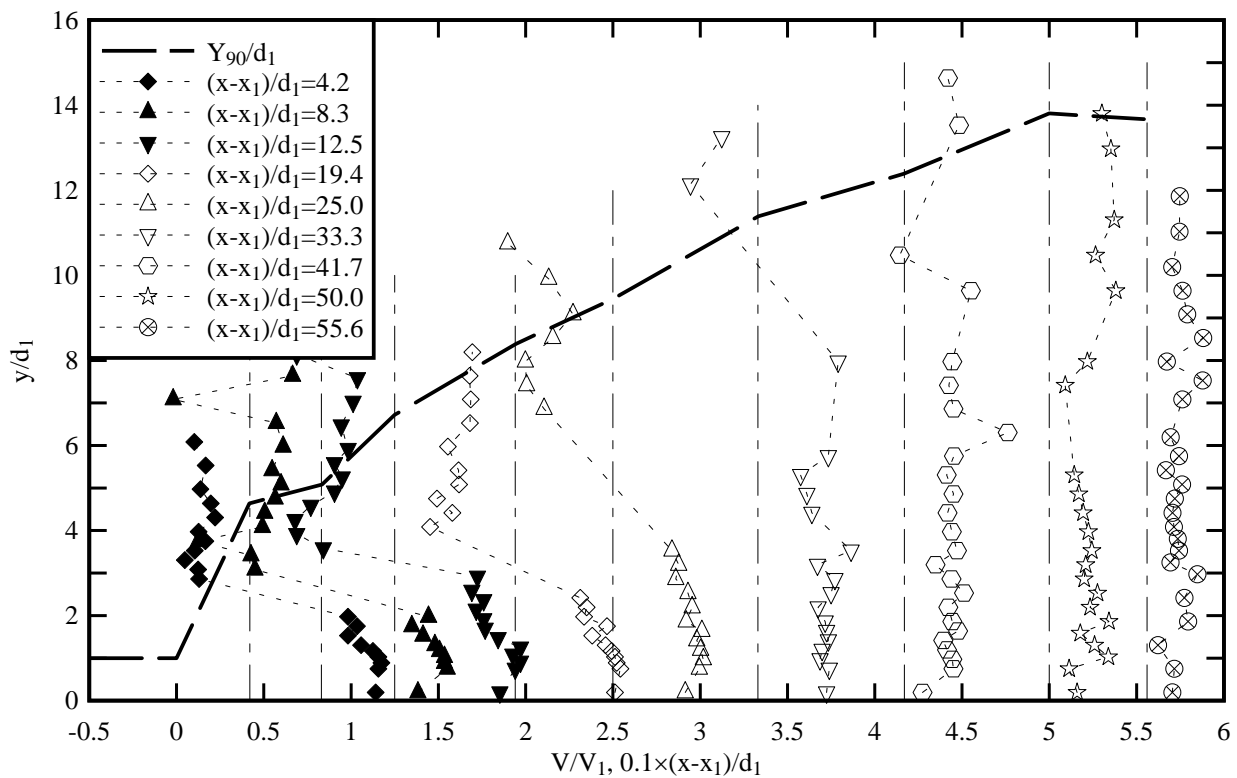
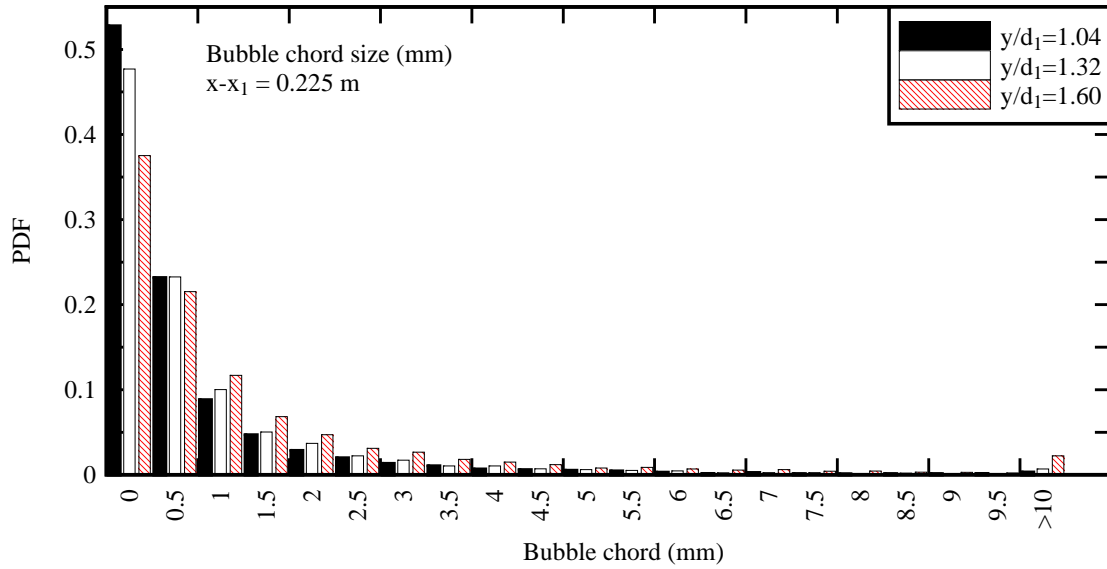
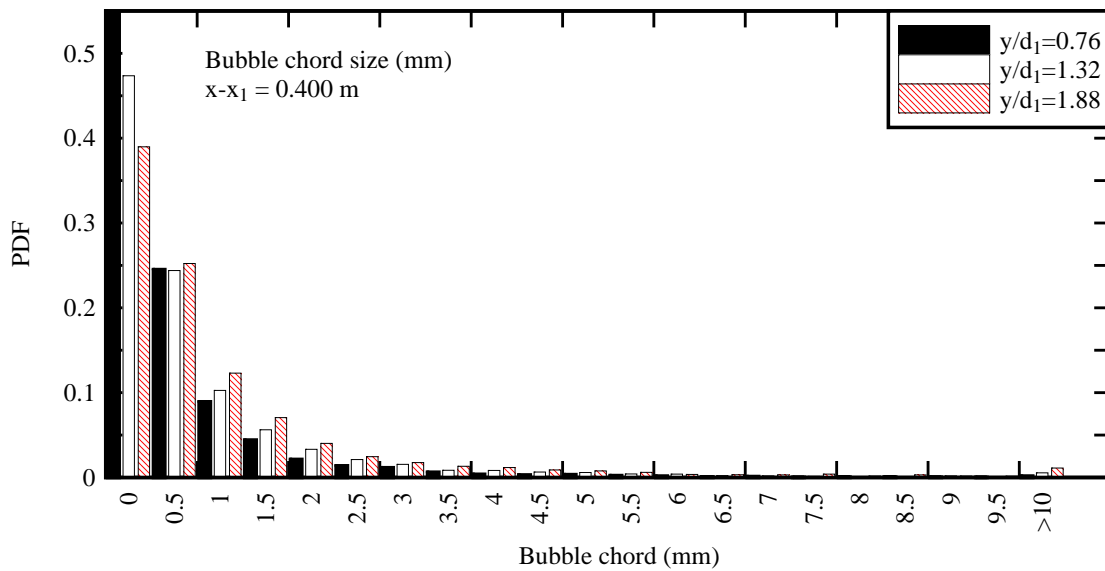


Fig. 9 - Probability distribution functions of bubble chords in the shear layer: $Fr_1 = 11.2$, $Re = 8.3 \times 10^4$, $d_1 = 0.01783$ m, $x_1 = 0.75$ m - Flow characteristics summarised in Table 2

(A) $x - x_1 = 0.225$ m



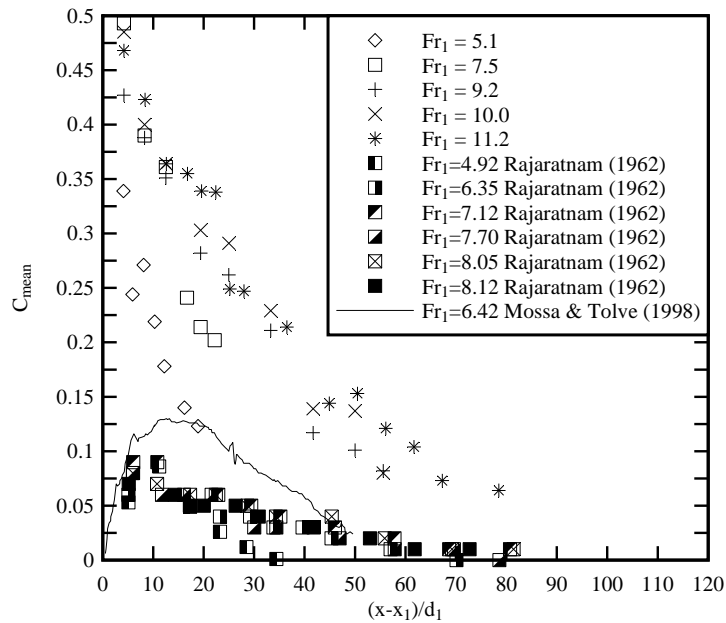
(B) $x - x_1 = 0.400$ m



CHANSON, H. (2011). "Bubbly Two-Phase Flow in Hydraulic Jumps at Large Froude Numbers." *Journal of Hydraulic Engineering*, ASCE, Vol. 137, No. 4, pp. 451-460 (DOI: 10.1061/(ASCE)HY.1943-7900.0000323) (ISSN 0733-9429).

Fig. 10 - Dimensionless longitudinal distributions of depth-averaged void fraction C_{mean} in hydraulic jumps

(A) Comparison between the present data and previous studies (Rajaratnam 1962, Mossa and Tolve 1998)



(B) Comparison between experimental data and Equation (7)

